KSME

Springer

Journal of Mechanical Science and Technology 34 (12) 2020

Original Article
DOI 10.1007/s12206-020-1107-2

Keywords:
· Fatigue driving energy
· Life estimation
· Material memory
· Nonlinear damage model
· Variable amplitude loading

Correspondence to:
Qiwen Xue
xueqiwen@djtu.edu.cn

Citation:
Xu, X., Xue, Q., He, Y. (2020). Nonlinear fatigue life prediction model based on material memory. Journal of Mechanical Science and Technology 34 (12) (2020) 5029~5039.
http://doi.org/10.1007/s12206-020-1107-2

Received December 27th, 2019
Revised August 17th, 2020
Accepted August 31st, 2020

† Recommended by Editor Chongdu Cho

© The Korean Society of Mechanical Engineers and Springer-Verlag GmbH Germany, part of Springer Nature 2020

# Nonlinear fatigue life prediction model based on material memory

Xu Xu[1], Qiwen Xue[1,2] and Yiqian He[2]

[1]School of Civil Engineering, Dalian Jiaotong University, Liaoning Dalian 116028, China, [2]State Key Laboratory of Structural Analysis for Industrial Equipment, Department of Engineering Mechanics, Dalian University of Technology, Dalian 116024, China

**Abstract** New nonlinear fatigue damage accumulation model is established on the basis of material memory theory and fatigue driving energy damage parameters to evaluate high-cycle fatigue life under multilevel variable amplitude loading. The loading interaction factor is constructed on the basis of damage degree and then the model is modified to consider the effect of loading interaction on fatigue damage accumulation. The two proposed models are convenient for calculation and have only two parameters that can be easily identified through experiments. In accordance with the test data of aluminum alloy Al-2024-T42, titanium alloy Ti-6Al-4V, nodular cast iron GS61, Q235B welded joint, and hot-rolled 16Mn steel, the two models developed in this study have been verified to predict fatigue life effectively. For multilevel loading, the modified model achieves higher prediction accuracy and its results are closer to the actual test data compared with those of the other models.

## 1. Introduction

To meet the development requirements of high speed, high power, and light weight, welding structures have become the mainstream of the mechanical manufacturing industry. Under the action of complex cyclic loading, welded structures are prone to fatigue failure and even sudden fracture during their usage process. Fatigue failure is one of the most frequently encountered problems in welded structures; it occurs in rail transit, shipbuilding, aerospace, and other engineering fields [1, 2]. Fatigue failure is invisible and unpredictable [3]. When welding fatigue occurs during the service operation of a mechanical structure, it will frequently result in heavy casualties and huge economic losses. To ensure the safe operation of a welded structure during its service life and avoid major accidents, studying the fatigue problem of welded structures is of considerable theoretical significance and engineering value.

Many experts have studied the fatigue problem of welded structures in recent years, and they have proposed a variety of fatigue life prediction methods that can be grouped into two major types: methods based on the S-N curve and fatigue damage accumulation theory and methods based on fracture mechanics theory [4, 5]. Numerous material parameters are necessary for prediction methods based on fracture mechanics theory, and these methods are difficult to measure. If the approximate value is used, then prediction accuracy will be affected. In addition, the calculation process under multilevel loading is complicated, and thus, difficult to use extensively in engineering problems. The required parameters can be obtained directly through fatigue experiments. These parameters are used in prediction methods based on the S-N curve and fatigue damage accumulation theory. Thus, prediction results exhibit high credibility. These methods are currently the mainstream for fatigue life prediction.

Fatigue damage accumulation theory can be divided into linear and nonlinear fatigue damage accumulation theories in accordance with different damage accumulation modes. For linear damage accumulation theory, the most widely used approach is the Palmgren–Miner linear fatigue damage accumulation rule, which exhibits the advantages of less parameters and a simple mathematical model [6]. However, the damage accumulation law of this rule is not related to stress level, and the prediction results tend to be highly deviated. A large number of calculation results show that loading sequence and loading interaction exert considerable influences on prediction results under multilevel variable amplitude loading; however, these factors are not considered in the Palmgren–Miner rule [7, 8]. Considering the deficiencies of linear damage accumulation models, researchers have presented a variety of nonlinear damage accumulation theories. Zhou et al. proposed a fatigue life prediction model based on material memory performance; this model requires less parameters and exhibits certain prediction accuracy [9]. Aeran et al. proposed a new fatigue life prediction model based on the S-N curve parameters of general materials; it does not require additional material parameter determination or S-N curve modification [10]. Zhu et al. proposed a new nonlinear fatigue damage accumulation model by introducing damage functions related to equal damage curve and residual life; this model considers the influence of loading history and improves calculation accuracy [11]. Nonlinear accumulation theory can consider the influences of loading sequence and loading interaction, improving prediction accuracy under multilevel loading. However, most nonlinear cumulation theoretical expressions are multilayer nesting. Thus, the calculation process is extremely complicated, and occasionally, additional unknown parameters should be introduced, further complicating the prediction process. These reasons make the model difficult to apply in engineering practice.

To solve the aforementioned problems, the authors of Ref. [12] proposed an effective fatigue life prediction method based on strain energy density parameters. This analysis method, which is based on the energy criterion concurring with the mechanism of fatigue fracture, has been widely used. In Ref. [12], the concept of fatigue driving energy was defined on the basis of strain energy density combined with the Basiquin formula and the Manson-Coffin equation. A prediction model was then proposed. The model can be used to evaluate fatigue life under high cyclic amplitude load. This nonlinear fatigue damage accumulation model exhibits the advantage of having a few parameters and these parameters have clear physical meanings. This model can consider the effects of loading sequence and loading interaction on the prediction results. However, the change in load amplitude under variable amplitude loading makes the damage accumulation rule extremely complicated. The evolution law of fatigue damage is closely related to the loading process. Loading sequence, loading interaction, material degradation, and other factors directly affect the law of damage evolution, and related research should be conducted further.

From the perspective of macro-mechanics, the accumulation process of fatigue damage can be regarded as the continuous degradation of the mechanical properties of materials [13]. However, determining the law of material performance degradation is frequently difficult, and the commonly used method is adopting a large number of actual data for fitting. In Refs. [14, 15], the authors simulated the process of human brain memory deterioration [16]. The material memory function was constructed by replacing the time parameter in the human brain memory function to simulate the material performance degradation law. The theory can accurately describe the degradation law of material properties, and it has only one parameter that can be easily determined through experiments without introducing other parameters. The mathematical model is simple and has broad application prospects.

At present, most fatigue damage accumulation models do not consider the effect of material performance degradation on damage accumulation. Models that consider this factor frequently have multiple parameters that are often not directly obtained by conducting a fatigue test, complicating the prediction process and reducing model versatility. The model proposed in Ref. [12] and material memory theory exhibit the advantages of less introduced parameters. If the two are combined, then the resulting model cannot only compensate for the deficiency of the model proposed in Ref. [12], which does not consider the material performance degradation mechanism, but will also not require introducing other redundant parameters to ensure universality.

On the basis of the aforementioned considerations, this study used material memory performance theory to modify the fatigue driving energy model and established an improved nonlinear fatigue life prediction model. The validity and feasibility of the developed fatigue life prediction model were verified using the fatigue data of aluminum alloy Al-2024-T42, titanium alloy Ti-6Al-4V, nodular cast iron GS61, and alloy welded joints. The results were then compared with those of other numerical models. The comparison of the numerical verification results indicates that the improved model can efficiently describe the degradation behavior of materials and effectively estimate their fatigue life under multilevel loading conditions with relatively high accuracy.

## 2. Model improvement

### 2.1 Nonlinear fatigue damage accumulation model

In accordance with the definition of fatigue driving energy in Ref. [12], the general formula for the life prediction of the fatigue driving energy model can be derived as follows.

For high cycle fatigue problems, the relationship between fatigue life and stress (i.e., the S-N curve) is frequently described using the Basquin formula [17]:

$$\sigma N_f^{-b} = C \tag{1}$$

where σ is the applied stress level, $C$ is the inherent fatigue strength constant of the material, $b$ is the material performance parameter, and $N_f$ is the fatigue life for the corresponding stress level. Instantaneous fatigue driving loading changes with fatigue load, and this condition is the primary cause of damage accumulation. It can be defined as the fatigue driving force. The expression is

$$\sigma_D = \sigma N_f^{-b\frac{n}{N_f}} \tag{2}$$

where $\sigma_D$ is the fatigue driving stress, and $n$ is the number of cycles at a given stress level. Strain energy density is commonly used to describe the fatigue failure process. Within the elastic range, the expression of strain energy density is [18]

$$W = \frac{1}{2}\sigma\varepsilon \tag{3}$$

where $W$ is the elastic strain energy density, and $\varepsilon$ is the elastic strain. The problem of high cycle fatigue is primarily controlled via cyclic stress. The corresponding elastic strain is dominant, and plastic strain can be disregarded. By combining the Basiquin formula with the Manson–Coffin equation [19], the relationship between total strain energy and fatigue life can be obtained as follows:

$$W_a = \frac{1}{2E}\sigma_a^2 \tag{4}$$

where $W_a$ is the amplitude of the elastic strain energy density, $E$ is the Young's modulus, and $\sigma_a$ is the applied stress amplitude. By substituting the fatigue driving force, i.e., Eq. (2), into the total strain energy, i.e., Eq. (4), the fatigue driving energy damage parameter model can be obtained as follows:

$$W_{D_n} = \frac{1}{2E}\sigma^2 N_f^{-2b\frac{n}{N_f}} \tag{5}$$

where $W_{Dn}$ is the fatigue driving energy. Determining the damage parameter is the core of fatigue damage accumulation theory. In Ref. [12], the damage parameter was defined by an increment in fatigue driving energy, and its expression can be written as follows:

$$D = \frac{\Delta W_{D_n,D_0}}{\Delta W_{D_c,D_0}} = \frac{W_{D_n} - W_{D_0}}{W_{D_c} - W_{D_0}} = \frac{N_f^{-2b\frac{n}{N_f}} - 1}{N_f^{-2b} - 1} \tag{6}$$

where $W_{D0}$ is the initial fatigue driving energy of the initial state when $n/N_f = 0$, and $W_{Dc}$ is the critical fatigue driving energy of the critical state at $n/N_f = 1$. Then, $\Delta W_{Dn,\,D0}$ is the energy dissipated by the actual load cycle, $\Delta W_{Dc,\,D0}$ is the total energy dissipated from the initial state to the failure state, and material parameter $b$ can be calculated using Eq. (1).

From Eq. (6), damage parameter $D$ is a nonlinear function related to the load cycle ratio. Thus, the model is a nonlinear damage accumulation model. In the evolution equation of the model, damage and load are inseparable parameters. Hence, the model can consider the effect of loading sequence. For multilevel loading, the calculation format of fatigue life prediction under $\sigma_i$ can be obtained through iterative calculation, as follows:

$$\left(\frac{n_i}{N_{f_i}}\right)_{pp} = 1 - \frac{1}{-2b\ln N_{f_i}} \cdot \ln\left[\frac{\left(N_{f_i}^{-2b} - 1\right)\left(N_{f(i-1)}^{-2b\left[\frac{n_{i-1}}{N_{f(i-1)}} + 1 - \left(\frac{n_{i-1}}{N_{f(i-1)}}\right)_{pp}\right]} - 1\right)}{N_{f(i-1)}^{-2b} - 1} + 1\right]. \tag{7}$$

Eq. (7) is the calculation formula for level i prediction life fraction. Considering that the loading interaction effect considerably influences fatigue damage accumulation, the model shown in Eq. (7) can be modified using the damage equivalent rule. Under multilevel loading, the stress ratio of two adjacent level loads can be used to correct the model. The modified residual fatigue life prediction model is as follows:

$$\left(\frac{n_i}{N_{f_i}}\right)_{pp} = 1 - \frac{1}{-2b\ln N_{f_i}} \cdot \ln\left[\left(N_{f_i}^{-2b} - 1\right)\left(\frac{N_{f(i-1)}^{-2b\left[\frac{n_{i-1}}{N_{f(i-1)}} + 1 - \left(\frac{n_{i-1}}{N_{f(i-1)}}\right)_{pp}\right]} - 1}{N_{f(i-1)}^{-2b} - 1}\right)^{\frac{\sigma_{i-2}}{\sigma_{i-1}} \times \frac{\sigma_i}{\sigma_{i-1}}} + 1\right]. \tag{8}$$

Eq. (8) is the fatigue driving energy model modified using the stress ratio. When the given model is used in fatigue life prediction, only two basic parameters ($b$ and $N_f$) should be determined. The values of the two parameters can be easily determined using the S-N curve obtained from the experiment. The introduction of other parameters is not required. The calculation model is relatively evident and direct, with good engineering application.

## 2.2 Modified model based on material memory

In accordance with Refs. [14, 15], the time function of the forgetting curve of the human brain is replaced with the loading cycle, and the material memory function can be obtained as follows:

$$M = \left(A_m - B_m\right)e^{-\frac{n}{d_m}} + B_m \tag{9}$$

where $M$ is the material memory performance; $A_m$ is the memorization rate; $B_m$ is the asymptote of the function; and $d_m$ is the reverse of the forgetting factor given in the number of cycles, which can be set as $d_m = N_f$.

In accordance with the memory function defined in the preceding equation, the attenuation coefficient can represent the degradation degree of a material, and its expression is

$$\alpha = \frac{M\big|_n - M\big|_{n=N_f}}{M\big|_{n=0} - M\big|_{n=N_f}} = \frac{\left[(A_m - B_m)e^{-\frac{n}{N_f}} + B_m\right] - \left[(A_m - B_m)e^{-1} + B_m\right]}{A_m - \left[(A_m - B_m)e^{-1} + B_m\right]} = \frac{e^{-\frac{n}{N_f}} - e^{-1}}{1 - e^{-1}} \tag{10}$$

where $\alpha$ is the degradation coefficient of material memory performance, the value range of which is [0, 1]. In the initial stage (when $n/N_f = 0$, $\alpha = 1$), the material is in a state without damage and no degradation occurs. With continuous loading action, material performance degrades gradually and α decreases continuously. Under critical condition (when $n/N_f = 1$, $\alpha = 0$), the material is in a state of complete degradation.

By introducing the attenuation coefficient in Eq. (10) into the fatigue driving force in Eq. (2), the modified fatigue driving force can be obtained, and its expression is as follows:

$$\sigma_D = \sigma N_f^{-b\alpha}. \tag{11}$$

By substituting the fatigue driving force, i.e., Eq. (11), into Eq. (5), the modified fatigue driving energy damage parameter model can be obtained as follows:

$$W_{D_n} = \frac{1}{2E}\sigma^2 N_f^{-2b\alpha} = \frac{1}{2E}\sigma^2 N_f^{-2b\frac{1-e^{-\frac{n}{N_f}}}{1-e^{-1}}}. \tag{12}$$

When $n/N_f$ regards 0 and 1 as two critical states, the value of $W_{Dn}$ after improvement is consistent with its previous value. The improved model conforms to the definition of the fatigue driving energy model, and the damage parameter expression of the modified model can be obtained in accordance with the previous derivation:

$$D = \frac{\Delta W_{D_n,D_0}}{\Delta W_{D_c,D_0}} = \frac{W_{D_n} - W_{D_0}}{W_{D_c} - W_{D_0}} = \frac{N_f^{-2b\alpha} - 1}{N_f^{-2b} - 1}. \tag{13}$$

The preceding equation shows that the damage parameter of the modified model is a nonlinear function related to load cycle ratio, and thus, this model is a nonlinear fatigue damage accumulation model. In the evolution equation of the modified model, load and damage are inseparable parameters, and loading sequence can be considered.

For a two-level block loading, the following equation can be derived in accordance with the equivalent damage rule:

$$D_1 = \frac{N_{f_1}^{-2b\alpha_1} - 1}{N_{f_1}^{-2b} - 1} = D_2' = \frac{N_{f_2}^{-2b\alpha_1'} - 1}{N_{f_2}^{-2b} - 1} \tag{14}$$

where $D_1$ is the damage of the first level load, $D'_2$ is the equivalent damage of the first level load to the second level load, $\alpha_1$ is the degradation coefficient of the first level load, and $\alpha'_1$ is the equivalent degradation coefficient of the first level load to the second level load. Then, the equivalent attenuation coefficient of the first level load can be deduced from the preceding equation as follows:

$$\alpha_1' = \frac{1}{-2b\ln N_{f_2}} \cdot \ln\left[1 + \frac{N_{f_2}^{-2b} - 1}{N_{f_1}^{-2b} - 1}\left(N_{f_1}^{-2b\alpha_1} - 1\right)\right]. \tag{15}$$

When the total damage of the two-level loading is equal to 1 (i.e., fatigue failure occurs), the following can be deduced:

$$D_2 = \frac{N_{f_2}^{-2b\left[\alpha_1' + (\alpha_2)_{pp}\right]} - 1}{N_{f_2}^{-2b} - 1} = 1. \tag{16}$$

That is,

$$\alpha_1' + (\alpha_2)_{pp} = 1. \tag{17}$$

By substituting Eq. (15) into Eq. (17), the predicted attenuation coefficient to the second level load $(\alpha_2)_{pp}$ can be obtained as follows:

$$(\alpha_2)_{pp} = 1 - \frac{1}{-2b\ln N_{f_2}} \cdot \ln\left[1 + \left(N_{f_2}^{-2b} - 1\right)\left(\frac{N_{f_1}^{-2b\alpha_1} - 1}{N_{f_1}^{-2b} - 1}\right)\right]. \tag{18}$$

By substituting Eq. (18) into Eq. (10), the calculation format of fatigue life prediction under the second level load can be obtained as follows:

$$\left(\frac{n_2}{N_{f_2}}\right)_{pp} = -\ln\left[1 - \left(1 - e^{-1}\right)\left(1 - \frac{1}{-2b\ln N_{f_2}} \cdot \ln\left[1 + \left(N_{f_2}^{-2b} - 1\right)\left(\frac{N_{f_1}^{-2b\alpha_1} - 1}{N_{f_1}^{-2b} - 1}\right)\right]\right)\right]. \tag{19}$$

For multilevel loading, Eq. (19) can be further extended to obtain the calculation format of life prediction under the *ith* level load:

$$\left(\frac{n_i}{N_{f_i}}\right)_{pp} = -\ln\left[1-\left(1-e^{-1}\right)\left(1-\frac{1}{-2b\ln N_{f_i}}\cdot \ln\left[1+\left(N_{f_i}^{-2b}-1\right)\left(\frac{N_{f_1}^{-2b\left(\alpha_{i-1}+\alpha'_{i-2}\right)}-1}{N_{f_1}^{-2b}-1}\right)\right]\right)\right] \tag{20}$$

where $\alpha_{i-1}$ is the attenuation coefficient of the (i−1)th level load, and $\alpha'_{-2}$ is the equivalent attenuation coefficient of the (i−2)th level load.

To consider the influence of loading interaction on fatigue life, the authors of Ref. [12] modified the original model by using the ratio of load sizes of two adjacent levels. However, under variable amplitude loading, the cumulative fatigue damage that corresponds to the failure is frequently not equal to 1. Low stress during the early stage exerts an initial exercise effect. Meanwhile, high stress during the early stage causes cracks to form in advance. If only the stress ratio is used to express the influence of load interaction, then the actual exercise degree of low stress and the formation state of high stress crack cannot be reflected. Some scholars have shown that the exercise effect of load can be described using real-time damage degree [20]. The authors of Ref. [20] proposed an interaction factor between loads based on the stress ratio of adjacent two-level loads and real-time damage degree; its feasibility was demonstrated through numerical examples. The mutual factors presented in Ref. [20] were introduced into the improved fatigue drive energy model for further modification.

In accordance with the modified method presented in Ref. [12], the interaction factor *m* between loads is substituted into Eq. (20) in exponential form to obtain

$$\left(\frac{n_i}{N_{f_i}}\right)_{pp} = -\ln\left[1-\left(1-e^{-1}\right)\left(1-\frac{1}{-2b\ln N_{f_i}}\cdot \ln\left[1+\left(N_{f_i}^{-2b}-1\right)\left(\frac{N_{f_1}^{-2b\left(\alpha_{i-1}+\alpha'_{i-2}\right)}-1}{N_{f_1}^{-2b}-1}\right)^{m}\right]\right)\right] \tag{21}$$

where

$$m = \beta_{i-1,i}\times\beta_{i-1,i-2}\ ,$$

$$\beta_{i-1,i} = \left(\frac{\sigma_i}{\sigma_{i-1}}\right)^{\exp(D_{i-1})},$$

$$\beta_{i-1,i-2} = \left(\frac{\sigma_{i-2}}{\sigma_{i-1}}\right)^{\exp(D_{i-2})}.$$

Table 1. Loading modes of the aluminum alloy Al-2024-T42 fatigue test.

| Loading mode | $\sigma_1$ (MPa) | $\sigma_2$ (MPa) | $n_1$ | $n_1/N_{f1}$ |
|---|---|---|---|---|
| 1 | 200 | 150 | 30000 | 0.200 |
| 2 | 200 | 150 | 60000 | 0.400 |
| 3 | 200 | 150 | 90000 | 0.600 |
| 4 | 150 | 200 | 86000 | 0.200 |
| 5 | 150 | 200 | 17200 | 0.400 |
| 6 | 150 | 200 | 25800 | 0.600 |

Eqs. (20) and (21) denote the improved fatigue driving energy model based on material memory theory and its modification model. Both models exhibit the advantages of less parameters and simple calculation. The modified model considers the influence of material degradation and effectively reflects the influences of loading sequence, interaction between loads, and real-time damage degree. Thus, the fatigue life of specimens can be evaluated more accurately under multilevel loading.

## 3. Numerical examples

The experimental data of aluminum alloy Al-2024-T42, titanium alloy Ti-6Al-4V, nodular cast iron GS61, the welding joint of the alloys, hot-rolled 16Mn steel, and Q235B welded joint are used to verify the feasibility of the modified model. The results are then compared with the results of the models presented in Refs. [9, 12]. The experimental data are normalized before calculation to prevent errors.

### *3.1 Comparative analysis of the prediction results of aluminum alloy Al-2024-T42 under two-level block loading*

Aluminum alloy Al-2024-T42 exhibits the advantages of high strength and high temperature resistance. It can produce various components that can bear high load, such as the skin, wing rib, and propeller, which are mostly used in the aerospace field. The comparison of the model prediction results and test data for aluminum alloy Al-2024-T42 at different stress levels and cycles are provided in Table 1 [21]. In the test, the fatigue life of the constant amplitude stress of high and low stress levels is $1.5\times10^5$ and $4.3\times10^5$ cycles, respectively.

The value of material parameter *b* can be calculated using Eq. (1) combined with the fatigue test data in Tables 1 and 2. The *b* value can be set as −0.273. For the model presented in Ref. [9], the recommended value for δ is −5.78.

From the comparison between the calculation results in Table 2 and Fig. 1, the nonlinear model established for aluminum alloy Al-2024-T42 in this study can effectively predict fatigue life under two-level block loading. The models from Refs. [9, 12] and the proposed model do not require the introduction of additional material parameters. Overall, however, the prediction accuracy of the proposed model is better compared with those of the other models. In the case with high–low loading se-

Table 2. Fatigue life prediction results of aluminum alloy Al-2024-T42.

| Mode | Experimental data | | Predicted value obtained using different models | | | |
|---|---|---|---|---|---|---|
| | $n_2$ | $n_2/N_{f2}$ | Miner rule | Ref. [9] model | Ref. [12] model | Proposed model |
| 1 | 228700 | 0.532 | 0.800 | 0.309 | 0.577 | 0.462 |
| 2 | 101050 | 0.235 | 0.600 | 0.182 | 0.419 | 0.401 |
| 3 | 76050 | 0.183 | 0.400 | 0.101 | 0.277 | 0.314 |
| 4 | 144500 | 0.963 | 0.800 | 0.999 | 0.967 | 0.840 |
| 5 | 133500 | 0.890 | 0.600 | 0.979 | 0.824 | 0.778 |
| 6 | 81700 | 0.545 | 0.400 | 0.887 | 0.574 | 0.215 |

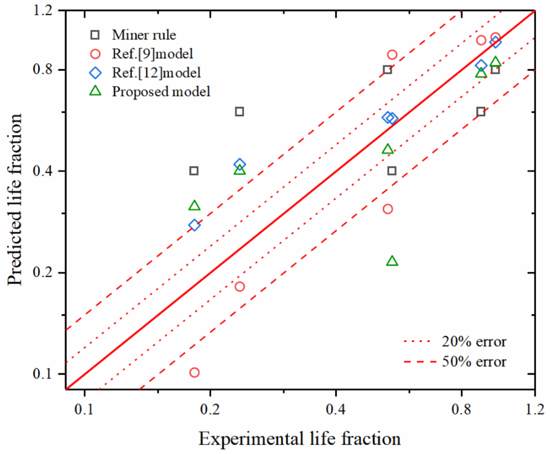


Fig. 1. Comparison of the fatigue life prediction results of aluminum alloy Al-2024-T42 obtained using different models.

quence, all the $n_1/N_{f1}+n_2/N_{f2}$ values calculated using the proposed model are less than 1; in the case of low–high loading sequence, all the $n_1/N_{f1}+n_2/N_{f2}$ values calculated using the proposed model are greater than 1. These results prove that the proposed model can accurately reflect the exercise effect of low stress and the acceleration effect of high stress on crack formation.

### 3.2 Comparative analysis of the prediction results of titanium alloy Ti-6Al-4V under two-level loading

Ti-6Al-4V is the first titanium alloy that was successfully developed and applied. It exhibits excellent heat resistance, corrosion resistance, strength, toughness, and biocompatibility. This alloy is primarily used in manufacturing the compressor components of aeroengines and the structural components of missiles and rockets. The comparison of the model prediction results and test data for titanium alloy Ti-6Al-4V at different stress levels and cycles are provided in Table 2 [22]. In the test, the fatigue life of the constant amplitude stress of the high and low stress levels is $8.3\times10^4$ and $3.7\times10^5$ cycles, respectively.

The value of material parameter *b* can be calculated using Eq. (1) combined with the fatigue test data provided in Tables 3 and 4. The *b* value can be set as −0.39. For the model presented in Ref. [9], the recommended value for δ is −5.78.

From the comparison between the calculation results in Table 4 and Fig. 2, the nonlinear model established for titanium

Table 3. Loading modes of the titanium alloy Ti-6Al-4V fatigue test.

| Loading mode | $\sigma_1$ (MPa) | $\sigma_2$ (MPa) | $n_1$ | $n_1/N_{f1}$ |
|---|---|---|---|---|
| 1 | 217 | 121 | 16500 | 0.199 |
| 2 | 217 | 121 | 20740 | 0.250 |
| 3 | 217 | 121 | 20740 | 0.250 |
| 4 | 217 | 121 | 33210 | 0.400 |
| 5 | 217 | 121 | 47300 | 0.570 |
| 6 | 217 | 121 | 62000 | 0.747 |
| 7 | 121 | 217 | 93000 | 0.250 |
| 8 | 121 | 217 | 186000 | 0.500 |
| 9 | 121 | 217 | 279000 | 0.750 |
| 10 | 121 | 217 | 298000 | 0.801 |

Table 4. Fatigue life prediction results of titanium alloy Ti-6Al-4V.

| Mode | Experimental data | | Predicted value obtained using different models | | | |
|---|---|---|---|---|---|---|
| | $n_2$ | $n_2/N_{f2}$ | Miner rule | Ref. [9] model | Ref. [12] model | Proposed model |
| 1 | 202145 | 0.543 | 0.800 | 0.070 | 0.404 | 0.300 |
| 2 | 94951 | 0.255 | 0.750 | 0.059 | 0.376 | 0.282 |
| 3 | 82900 | 0.223 | 0.750 | 0.059 | 0.376 | 0.282 |
| 4 | 107566 | 0.289 | 0.600 | 0.037 | 0.297 | 0.237 |
| 5 | 126142 | 0.339 | 0.430 | 0.021 | 0.212 | 0.178 |
| 6 | 46440 | 0.125 | 0.253 | 0.010 | 0.124 | 0.106 |
| 7 | 77646 | 0.936 | 0.750 | 1.000 | 0.999 | 0.858 |
| 8 | 52863 | 0.637 | 0.500 | 0.998 | 0.929 | 0.557 |
| 9 | 50745 | 0.612 | 0.250 | 0.996 | 0.508 | 0.284 |
| 10 | 32000 | 0.386 | 0.386 | 0.988 | 0.405 | 0.228 |

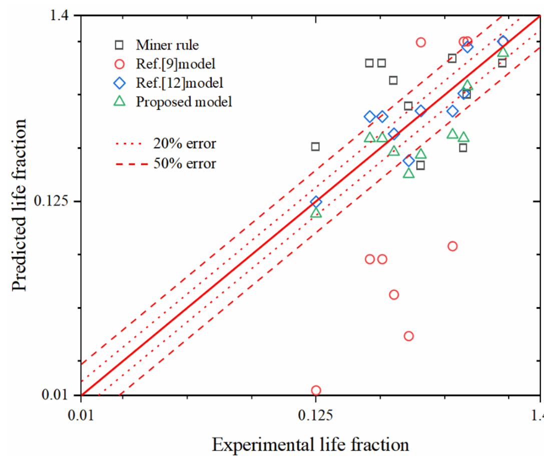


Fig. 2. Comparison of the fatigue life prediction results of titanium alloy Ti-6Al-4V obtained using different models.

Table 5. Loading modes of the ductile iron GS61 fatigue test.

| Loading type | Loading mode | $\sigma_1$ (MPa) | $\sigma_2$ (MPa) | $n_1$ | $n_1/N_{f1}$ |
|---|---|---|---|---|---|
| Plane bending loading | 1 | 352 | 320 | 50000 | 0.443 |
| | 2 | 352 | 303 | 50000 | 0.443 |
| | 3 | 320 | 352 | 110000 | 0.341 |
| | 4 | 303 | 352 | 160000 | 0.272 |
| Torsional loading | 1 | 249 | 233 | 50000 | 0.417 |
| | 2 | 233 | 249 | 160000 | 0.535 |

Table 6. Fatigue life prediction results of ductile iron GS61.

| Loading type | Loading mode | Experimental data | | Predicted value obtained using different models | | | |
|---|---|---|---|---|---|---|---|
| | | $n_2$ | $n_2/N_{f2}$ | Miner rule | Ref. [9] model | Ref. [12] model | Proposed model |
| Plane bending loading | 1 | 130510 | 0.405 | 0.557 | 0.392 | 0.494 | 0.438 |
| | 2 | 205040 | 0.349 | 0.557 | 0.312 | 0.459 | 0.275 |
| | 3 | 82830 | 0.734 | 0.659 | 0.823 | 0.725 | 0.819 |
| | 4 | 116650 | 1.030 | 0.728 | 0.935 | 0.824 | 0.677 |
| Torsional loading | 1 | 154270 | 0.516 | 0.583 | 0.440 | 0.534 | 0.494 |
| | 2 | 46310 | 0.386 | 0.456 | 0.584 | 0.507 | 0.516 |

alloy Ti-6Al-4V in this study can effectively predict fatigue life under two-level block loading. The models from Refs. [9, 12] and the proposed model do not require the introduction of additional material parameters. Overall, however, the prediction accuracy of the proposed model is better compared with those of the other models. In the case with high–low loading sequence, all the $n_1/N_{f1}+n_2/N_{f2}$ values calculated using the proposed model are less than 1; in the case with low–high loading sequence, all the $n_1/N_{f1}+n_2/N_{f2}$ values calculated using the proposed model are greater than 1.

## 3.3 Comparative analysis of the prediction results of ductile iron GS61 under two-level loading

Ductile iron GS61 is a high-strength, high-plasticity, and high-toughness cast iron material. The mechanical properties of cast iron are considerably improved after spheroidization and inoculation. Ductile iron GS61 is primarily used to manufacture various complicated bearing parts, such as the camshafts and crankshafts of automobiles and internal combustion engines. The value of material parameter $b$ can be calculated using Eq. (1) combined with the fatigue test data provided in Tables 5 and 6 [23]. For plane bending loading, $b$ can be set as −0.09; for torsional loading, $b$ can be set as −0.073. For the model presented in Ref. [9], the recommended value for δ is −5.78.

From the comparison between the calculation results in Table 6 and Fig. 3, the nonlinear model for ductile iron GS61 established in this study can effectively predict fatigue life under two-level loading. The models presented in Refs. [9, 12] and the proposed model do not require the introduction of additional material parameters. Overall, however, the prediction accuracy of the proposed model is better compared with those of the other models. In the case with high–low loading sequence, all the $n_1/N_{f1}+n_2/N_{f2}$ values calculated using the proposed model are less than 1; in the case with low–high loading sequence, all the $n_1/N_{f1}+n_2/N_{f2}$ values calculated using the proposed model are greater than 1.

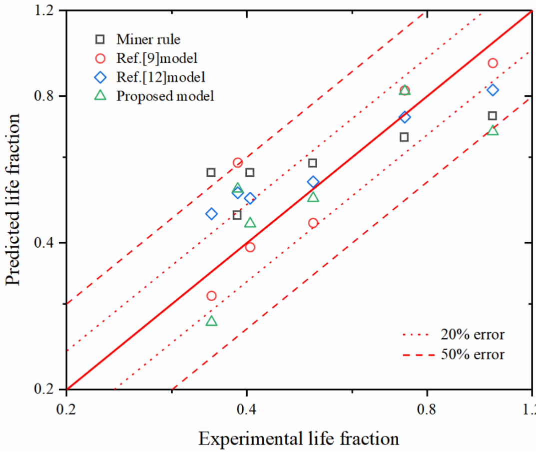


Fig. 3. Comparison of the fatigue life prediction results of ductile iron GS61 obtained using different models.

## 3.4 Comparative analysis of the prediction results of butt- and fillet-welded joints under two-level loading

Aluminum alloy materials exhibit the advantages of light weight, high strength, good plasticity, good heat conductivity, and high corrosion resistance. They are ideal materials for manufacturing all types of welded structural parts. For the butt- and fillet-welded joints of the aluminum alloy body of high-speed extravehicular mobility units, the comparison of the model prediction results and test data at different stress levels and cycles are provided in Table 4 [24]. The value of material parameter $b$ can be calculated using Eq. (1) combined with the fatigue test data provided in Tables 7 and 8. For the butt-welded joint, $b$ can be set as −0.33; for the fillet-welded joint, $b$ can be set as −0.265.

From the comparison between the calculation results in Table 8 and Fig. 4, the nonlinear model for butt- and fillet- welded joints established in this study can effectively predict fatigue life under two-level loading. Overall, the prediction accuracy of the proposed model is better compared with those of the two other models. In the case of high–low loading sequence, all the $n_1/N_{f1}+n_2/N_{f2}$ values calculated using the proposed model are less than 1; in the case of low–high loading sequence, all the $n_1/N_{f1}+n_2/N_{f2}$ values calculated using the proposed model are greater than 1.

Table 7. Loading modes of the butt- and fillet-welded joint fatigue test.

| Welding type | Loading mode | $\sigma_1$ (MPa) | $\sigma_2$ (MPa) | $n_1$ | $n_1/N_{f1}$ |
|---|---|---|---|---|---|
| Butt joint | 1 | 104 | 74 | 109900 | 0.200 |
| | 2 | 89 | 74 | 176100 | 0.200 |
| | 3 | 74 | 89 | 770100 | 0.500 |
| | 4 | 74 | 104 | 770100 | 0.500 |
| Corner joint | 1 | 93 | 73 | 309900 | 0.500 |
| | 2 | 83 | 73 | 476100 | 0.499 |
| | 3 | 73 | 83 | 509200 | 0.329 |
| | 4 | 73 | 93 | 773000 | 0.500 |

Table 8. Fatigue life prediction results of butt- and fillet-welded joints.

| Welding type | Loading mode | Experimental data | | Predicted value obtained using different models | | | |
|---|---|---|---|---|---|---|---|
| | | $n_2$ | $n_2/N_{f2}$ | Miner rule | Ref. [9] model | Ref. [12] model | Proposed model |
| Butt joint | 1 | 797600 | 0.518 | 0.800 | 0.243 | 0.541 | 0.456 |
| | 2 | 1029200 | 0.668 | 0.800 | 0.470 | 0.651 | 0.615 |
| | 3 | 545600 | 0.620 | 0.500 | 0.826 | 0.639 | 0.855 |
| | 4 | 418900 | 0.763 | 0.500 | 0.978 | 0.740 | 0.651 |
| Corner joint | 1 | 587500 | 0.380 | 0.500 | 0.174 | 0.370 | 0.413 |
| | 2 | 681100 | 0.441 | 0.500 | 0.298 | 0.426 | 0.581 |
| | 3 | 708200 | 0.744 | 0.671 | 0.878 | 0.772 | 0.818 |
| | 4 | 426400 | 0.688 | 0.500 | 0.903 | 0.670 | 0.668 |

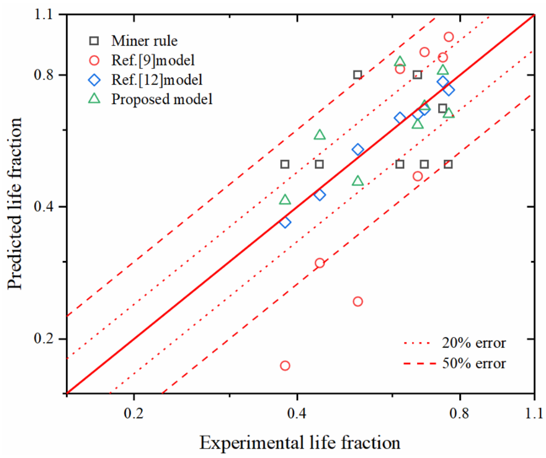


Fig. 4. Comparison of the fatigue life prediction results of butt- and fillet-welded joints obtained using different models.

## 3.5 Comparative analysis of the prediction results of hot-rolled 16Mn steel under two-level loading

Hot-rolled 16Mn steel is an excellent structural steel with high strength, good toughness, good welding performance, and other characteristics; it is widely used in modern engineering. The comparison of the model prediction results and test data for hot-rolled 16Mn steel at different stress levels and

Table 9. Loading modes of hot-rolled 16Mn steel.

| Loading mode | $\sigma_1$ (MPa) | $\sigma_2$ (MPa) | $n_1$ | $n_1/N_{f1}$ |
|---|---|---|---|---|
| 1 | 394 | 345 | 9350 | 0.100 |
| 2 | 394 | 345 | 19700 | 0.211 |
| 3 | 394 | 345 | 39400 | 0.421 |
| 4 | 394 | 345 | 46750 | 0.500 |
| 5 | 394 | 345 | 56100 | 0.600 |
| 6 | 345 | 394 | 181000 | 0.450 |
| 7 | 345 | 394 | 197100 | 0.490 |
| 8 | 345 | 394 | 233300 | 0.580 |

Table 10. Fatigue life prediction results of hot-rolled 16Mn steel.

| Mode | Experimental data | | Predicted value obtained using different models | | | |
|---|---|---|---|---|---|---|
| | $n_2$ | $n_2/N_{f2}$ | Miner rule | Ref. [9] model | Ref. [12] model | Proposed model |
| 1 | 269500 | 0.670 | 0.900 | 0.695 | 0.834 | 0.560 |
| 2 | 236100 | 0.587 | 0.789 | 0.551 | 0.701 | 0.411 |
| 3 | 209500 | 0.521 | 0.579 | 0.352 | 0.490 | 0.250 |
| 4 | 159300 | 0.396 | 0.500 | 0.292 | 0.418 | 0.200 |
| 5 | 74000 | 0.184 | 0.400 | 0.222 | 0.330 | 0.150 |
| 6 | 82867 | 0.886 | 0.550 | 0.786 | 0.641 | 0.629 |
| 7 | 80970 | 0.866 | 0.510 | 0.748 | 0.600 | 0.581 |
| 8 | 59570 | 0.637 | 0.420 | 0.654 | 0.501 | 0.285 |

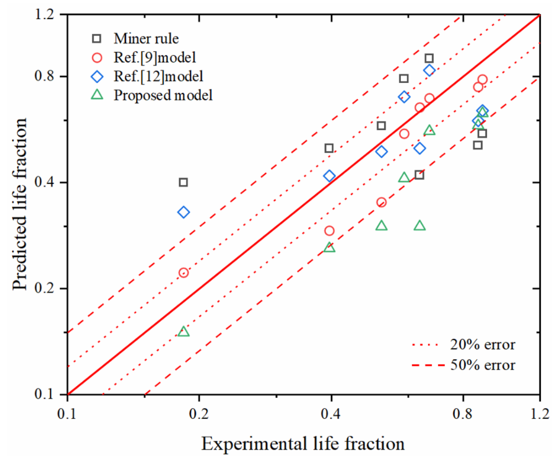


Fig. 5. Comparison of the fatigue life prediction results of hot-rolled 16Mn steel obtained using different models.

cycles are provided in Table 9 [25]. In the test, the fatigue life of the constant amplitude stress at high and low stress levels is $9.3\times10^4$ and $4.0\times10^5$ cycles, respectively.

The value of material parameter $b$ can be calculated using Eq. (1) combined with the fatigue test data provided in Tables 9 and 10. The $b$ value can be set as −0.09. For the model presented in Ref. [9], the recommended value for δ is −5.78.

From the comparison between the calculation results in Ta-

Table 11. Loading modes of the Q235B welded joint fatigue test.

| Loading level | Loading mode | $\sigma_i$ (MPa) | $n_i$ |
|---|---|---|---|
| Three-level loading | 1 | 38.00 | 40.00 |
| | | 40.00 | 40.00 |
| | | 42.00 | 24.75 |
| | 2 | 40.00 | 40.00 |
| | | 42.00 | 40.00 |
| | | 44.00 | 27.63 |
| | 3 | 20.00 | 49.60 |
| | | 21.50 | 50.30 |
| | | 22.40 | 10.68 |
| Four-level loading | 1 | 20.60 | 49.60 |
| | | 21.50 | 50.30 |
| | | 22.40 | 40.60 |
| | | 23.30 | 39.94 |
| | 2 | 28.95 | 40.00 |
| | | 30.48 | 40.00 |
| | | 32.00 | 40.00 |
| | | 35.05 | 8.24 |
| | 3 | 30.48 | 40.00 |
| | | 33.52 | 40.00 |
| | | 35.05 | 40.00 |
| | | 38.10 | 14.05 |

ble 10 and Fig. 5, the nonlinear model for hot-rolled 16Mn steel established in this study can effectively predict fatigue life under two-level block loading. The models presented in Refs. [9, 12] and the proposed model do not require the introduction of additional material parameters. Overall, however, the prediction accuracy of the proposed model is better compared with those of the other models.

### 3.6 Comparative analysis of the prediction results of Q235B welded joint under multilevel loading

Q235B is a common welding material for the welded frames of railway vehicle bogies. The experimental data of Q235B welded joints under multilevel variable amplitude loading in the literature are used to verify the fatigue life prediction capability of the modified model. The comparison between the model prediction results and the test data at different stress levels and cycles is presented in Tables 11 and 12 [26].

From the calculation results in Tables 11 and 12 and Fig. 6, the two nonlinear fatigue life prediction models developed in this study can effectively predict the fatigue life of Q235B welded joints under multilevel variable amplitude loading. Compared with the Miner rule and the results of the models presented in Refs. [9, 12], the prediction accuracy of the two nonlinear models proposed in this study is improved to a certain extent. For example, the prediction results of the modified

Table 12. Fatigue life prediction results of Q235B welded joint under multi-level loading.

| Loading level | Mode | Experimental life | Predicted fatigue life using different models | | | | |
|---|---|---|---|---|---|---|---|
| | | $N_E/10^4$ | Miner rule | Ref. [9] model | Ref. [12] model | Proposed model | Modified model |
| Three | 1 | 104.75 | 88.20 | 102.6 | 94.01 | 120.95 | 118.58 |
| | 2 | 107.63 | 71.01 | 84.1 | 62.80 | 115.33 | 112.94 |
| | 3 | 110.58 | 151.44 | 160.5 | 148.14 | 166.96 | 116.57 |
| Four | 1 | 180.44 | 129.57 | 160.3 | 146.80 | 148.83 | 160.15 |
| | 2 | 128.24 | 112.45 | 136.3 | 120.24 | 123.24 | 114.99 |
| | 3 | 134.05 | 78.26 | / | / | 123.98 | 132.40 |

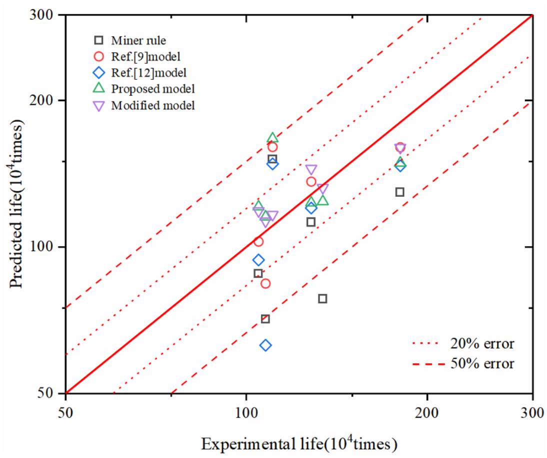


Fig. 6. Comparison of the fatigue life prediction results of Q235B welded joint under multilevel loading obtained using different models.

model are closer to the actual experimental data, indicating that the interaction factors constructed on the basis of damage degree can effectively reflect the impact of load interaction on damage accumulation.

## 4. Conclusions

1) A new nonlinear fatigue life prediction model and its modified version are established. Material memory performance theory and real-time damage degree are used to modify the driving energy model. The modified model can accurately analyze the fatigue life of welded structures and effectively address the influences of relevant factors on the damage evolution law of variable amplitude loading without introducing additional parameters.

2) From the calculation results of three alloy materials, the proposed model is feasible under two-level block loading. Compared with the models presented in Refs. [9, 12], which also do not require the introduction of additional parameters, the life prediction accuracy of the proposed model is higher, enabling it to better solve the fatigue problem in engineering.

3) From the calculation results of two types of welded joints,

the two models proposed in this study can better evaluate the fatigue life of welded structures compared with the models presented in Refs. [9, 12]. Solving the fatigue problem of welding structures that frequently occurs in engineering is highly significant.

4) The proposed and modified models involve only two parameters, which are easy to determine through experiments. The recurrence scheme is also easy to implement. Therefore, the two models proposed in this work can be more widely applied to the life evaluation of practical engineering structures.

5) The calculation examples provided in this study are all block loadings. Although the feasibility of the proposed model can be proven, a certain difference exists between this model and the load suffered by components in actual engineering. In subsequent research, further work will be conducted on the basis of the two proposed models combined with loads in actual projects.

## Acknowledgments

This work was supported by the National Natural Science Foundation of China (Nos. 10802015, 11572077, and 11902062); the Natural Science Foundation of Liaoning Province (No.2019KF0204); the Liaoning Province Graduate Education and Teaching Reform Project (2017); and the State Key Laboratory of Structural Analysis for Industrial Equipment Open Funding, Dalian University of Technology (GZ19204).

## Nomenclature

$b$ : Material constant
$C$ : Fatigue strength constant
$D$ : Damage variable
$E$ : Young's modulus
$N$ : Number of cycles at a given stress level
$N_f$ : Number of cycles to failure
$N_E$ : Experimental fatigue life
$W$ : Elastic strain energy density
$W_a$ : Amplitude of elastic strain energy density
$W_{Dn}$ : Fatigue driving energy
$W_{D0}$ : Initial fatigue driving energy
$\Sigma$ : Applied stress level
$\sigma_D$ : Fatigue driving stress
$\sigma_a$ : Applied stress amplitude
$\varepsilon$ : Elastic strain
$M$ : Volume of memorized information
$A_m$ : Memorization rate
$B_m$ : Asymptote
$M$ : Loading interaction factor

## References

[1] S. R. Prasad and A. S. Sekhar, Life estimation of shafts using vibration based fatigue analysis, *Journal of Mechanical Science and Technology*, 32 (9) (2018) 4071-4078.

[2] R. Wang and P. Mi, Study on fatigue strength of FSW joints of 5083 aluminum alloy with kissing bond defect, *Journal of Mechanical Science and Technology*, 34 (7) (2020) 2761-2766.

[3] C. Mi, J. Liu and X. Xiao, Random vibration fatigue life assessment and optimization of a train buffer beam considering welding residual stress, *Journal of Mechanical Science and Technology* (2020) 1-10.

[4] D. G. Pavlou, The theory of the SN fatigue damage envelope: generalization of linear, double-linear and non-linear fatigue damage models, *International Journal of Fatigue*, 110 (2018) 204-214.

[5] J. P. Dias, S. Ekwaro-Osire and A. Cunha Jr., Parametric probabilistic approach for cumulative fatigue damage using double linear damage rule considering limited data, *International Journal of Fatigue*, 127 (2019) 246-258.

[6] M. A. Miner, Cumulative damage in fatigue, *Journal of Applied Mechanics*, 12 (3) (1945) 159-164.

[7] Z. Ma, P. Le Tallec and H. Maitournam, An energy-based strategy for fatigue analysis in presence of general multi-axial time varying loadings, *International Journal of Fatigue*, 132 (2020) 105367.

[8] F. Mozafari, P. Thamburaja and A. Srinivasa, Fatigue life prediction under variable amplitude loading using a microplasticity-based constitutive model, *International Journal of Fatigue*, 134 (2020) 105477.

[9] J. Zhou, H. Z. Huang and M. V. Barnhart, A novel non-linear cumulative fatigue damage model based on the degradation of material memory, *International Journal of Damage Mechanics*, 29 (4) (2020) 610-625.

[10] A. Aeran, S. C. Siriwardane and O. Mikkelsen, A new nonlinear fatigue damage model based only on SN curve parameters, *International Journal of Fatigue*, 103 (2017) 327-341.

[11] S. P. Zhu, D. Liao and Q. Liu, Nonlinear fatigue damage accumulation: isodamage curve-based model and life prediction aspects, *International Journal of Fatigue*, 128 (2019) 105185.

[12] Z. Peng, H. Z. Huang, S. P. Zhu, H. Gao and Z. Lv, A fatigue driving energy approach to high- cycle fatigue life estimation under variable amplitude loading, *Fatigue and Fracture of Engineering Materials and Structures*, 39 (2) (2016) 180-193.

[13] R. Yuan, H. Li, H. Z. Huang, S. P. Zhu and H. Gao, A nonlinear fatigue damage accumulation model considering strength degradation and its applications to fatigue reliability analysis, *International Journal of Damage Mechanics*, 24 (5) (2015) 646-662.

[14] E. Böhm, M. Kurek, G. Junak, M. Cieśla and T. Łagoda, Accumulation of fatigue damage using memory of the material, *Procedia Materials Science*, 3 (2014) 2-7.

[15] E. Böhm, M. Kurek and T. Łagoda, Fatigue damage accumulation model of 6082-T6 aluminum alloy in conditions of block bending and torsion, *Journal of Testing and Evaluation*, 48 (6) (2020).

[16] H. Ebbinghaus, *Memory: A Contribution to Experimental Psychology,* H. A. Ruger and C. E. Bussenius Translation, Teachers College, Columbia University, New York (1913).

[17] A. R. C. Murthy, G. S. Palani and N. R. Iyer, State-of-the-art

review on fatigue crack growth analysis under variable amplitude loading, *Journal of the Institution of Engineers India. Civil Engineering Division*, 85 (2004) 118-129.
[18] T. Łagoda, Energy models for fatigue life estimation under uniaxial random loading, part I: the model elaboration, *International Journal of Fatigue*, 23 (6) (2001) 467-480.
[19] Y. Hu, Z. Hu and S. Cao, Theoretical study on Manson-Coffin equation for physically short cracks and lifetime prediction, *Science China Technological Sciences*, 55 (1) (2012) 34-42.
[20] Q. W. Xue, X. Xu and S. W. Wang, Nonlinear fatigue life prediction analysis based on damage parameter correction, *China Railway Science*, 41 (2) (2020) 99-105 (in Chinese).
[21] D. G. Pavlou, A phenomenological fatigue damage accumulation rule based on hardness increasing, for the 2024-T42 aluminum, *Engineering Structures*, 24 (11) (2002) 1363-1368.
[22] O. Jin, H. Lee and S. Mall, Investigation into cumulative damage rules to predict fretting fatigue life of Ti-6Al-4V under two-level block loading condition, *Journal of Engineering Materials and Technology*, 125 (3) (2003) 315-323.
[23] A. Aïd, A. Amrouche, B. B. Bouiadjra, M. Benguediab and G. Mesmacque, Fatigue life prediction under variable loading based on a new damage model, *Materials and Design*, 32 (1) (2011) 183-191.
[24] J. Tian, Z. M. Liu and R. He, Nonlinear fatigue-cumulative damage model for welded aluminum alloy joint of EMU, *Journal of the China Railway Society*, 34 (3) (2012) 40-43.
[25] M. J. Zhou and H. Wang, Study on stress interaction of LZ50 steel under variable amplitude load, *Advanced Engineering Sciences*, S2 (2012) 57-59 (in Chinese).
[26] H. Gao, H. Z. Huang, S. P. Zhu, Y. F. Li and R. Yuan, A modified nonlinear damage accumulation model for fatigue life prediction considering load interaction effects, *The Scientific World Journal* (2014) 1-7.

**Xu Xu** is a postgraduate student in Dalian Jiaotong University, Dalian, China. His research interests include fatigue life calculation and damage mechanics.